JOURNAL OF VIROLOGY, May 2006, p. 5065–5073 Vol. 80, No. 10
0022-538X/06/$08.00+0 doi:10.1128/JVI.80.10.5065–5073.2006

The ORF3 Protein of Porcine Circovirus Type 2 Is Involved in Viral Pathogenesis In Vivo

Jue Liu, Isabelle Chen, Qingyun Du, Huikheng Chua, and Jimmy Kwang*

Animal Health Biotechnology Group, Temasek Life Sciences Laboratory, The National University of Singapore, 1 Research Link, Singapore 117604

Received 15 December 2005/Accepted 1 February 2006

Porcine circovirus type 2 (PCV2) is the primary causative agent of an emerging swine disease, postweaning multisystemic wasting syndrome. We previously showed that a novel identified protein, ORF3, was not essential for PCV2 replication in cultured PK15 cells and played a major role in virus-induced apoptosis. To evaluate the role of the ORF3 protein in viral pathogenesis in vivo, we inoculated 8-week-old BALB/c mice that have been developed for PCV2 replication with ORF3-deficient mutant PCV2 (mPCV2). By 42 days postinoculation, all of the mice inoculated with the mPCV2, as well as with wild-type PCV2 (wPCV2), had seroconverted to PCV2 capsid antibody, and the mutant induced levels of PCV2 antibodies that were higher than those of the wPCV2. The PCV2 genomic copy numbers in serum were significantly higher ($P < 0.05$) in the wPCV2-inoculated mice than in mice inoculated with the mPCV2. Also, the wPCV2 caused microscopic lesions characterized by lymphocyte depletion with histiocytic infiltration of lymphoid organs, but the mutant virus failed to induce any obvious pathological lesions. In situ hybridization and immunohistochemical analyses also showed that larger amounts of viral DNA and antigens were detected in the lymph nodes of the wPCV2-inoculated than mPCV2-inoculated mice. Furthermore, animals of the wPCV2-inoculated group showed significant downshifts of $CD8^+$ T-cell subsets of peripheral blood lymphocytes compared to the control mice ($P < 0.05$) at various time points postinoculation. Also, the proportions of the $CD4^+$ and $CD4^+$ $CD8^+$ cells were significantly reduced in wPCV2-inoculated mice at some time points postinoculation. In contrast, there are some reductions in the proportions of these subsets in the mutant virus-inoculated mice, but the proportions do not decrease significantly. Taken together, these results demonstrate that the ORF3 protein is also dispensable for viral replication in vivo and that it plays an important role in viral pathogenesis.

Infection with porcine circovirus type 2 (PCV2), but not PCV1, has been associated with postweaning multisystemic wasting syndrome (PMWS) in young weaned pigs. The disease was first recognized in Canada in 1991 (8) and has since been described in virtually all regions of the world that produce pigs (4, 7, 13, 16, 31, 37). Usually PMWS appears in pigs aged 5 to 18 weeks, and affected pigs show wasting or unthriftiness, respiratory distress, enlarged lymph nodes and, occasionally, jaundice and diarrhea (20, 44). Gross lesions in affected pigs consist of generalized lymphadenopathy in combination with interstitial pneumonia, hepatitis, renomegaly, splenomegaly, gastric ulcers, and intestinal wall edema (8, 21). The most distinct microscopic lesions are lymphoid cell depletion and granulomatous inflammation in lymphoid organs, with inconsistently occurring clusters of intensely basophilic intracytoplasmic inclusion bodies in macrophages (8, 14, 21, 25).

Porcine circovirus (PCV) is classified in the genus *Circovirus* of the *Circoviridae* family (38). The PCV virion is icosahedral, nonenveloped, and 17 nm in diameter. The genome of PCV is a single-stranded circular DNA of about 1.76 kb. The overall DNA sequence homology within the PCV1 or PCV2 isolates is greater than 90%, whereas the homology between PCV1 and PCV2 isolates is 68 to 76%. Two major open reading frames (ORFs) have been recognized for PCV, ORF1, called the *rep* gene, which encodes a protein of 35.7 kDa involved in virus replication (32), and ORF2, called the *cap* gene, which encodes the major immunogenic capsid protein of 27.8 kDa (6, 33). In addition to the replicase ORF1 and the capsid protein ORF2, we identified a novel protein, ORF3, in cultured PK15 cells during PCV2 productive infection and found that it is not essential for PCV2 replication in cultured cells (28). After analyzing genomic sequences of different geographic PCV2 strains, Larochelle et al. (27) speculated that a link between capsid protein variation and pathogenicity of PCV2 may exist due partly to alterations of the determinants involved in tissue tropism or virus-host interactions. Furthermore, P110A and R191S mutations in the capsid of PCV2 have also been demonstrated to enhance the growth ability of PCV2 in vitro and attenuate the virus in vivo after 120 passages in cultured PK15 cells (19). However, other regions outside the capsid might be also involved in viral pathogenesis when chimeric PCV1-2 virus with the immunogenic ORF2 capsid gene of pathogenic PCV2 cloned into the nonpathogenic PCV1 genomic backbone induced a specific antibody response to the pathogenic PCV2 capsid antigen but is attenuated in pigs (18). These research findings suggest that PCV2 pathogenesis is complicated and multigenic.

PCV1 viruses are naturally nonpathogenic and do not cause any pathological lesions in pigs (3, 46). By comparing to PCV2 ORF3 gene, we find that the corresponding region of PCV1 strains appears to be different and shows ca. 61.5% amino acid sequence identity to that of PCV2 (data not shown). PCV2 has been demonstrated to induce apoptosis in cultured PK15 cells

* Corresponding author. Mailing address: Animal Health Biotechnology Group, Temasek Life Sciences Laboratory, The National University of Singapore, 1 Research Link, Singapore 117604. Phone: (65) 68727473. Fax: (65) 68727007. E-mail: kwang@tll.org.sg.

via the ORF3 protein (28). Virus-induced apoptosis plays an important role in the pathogenesis of virus infection (40). However, whether the ORF3 protein is directly involved in PCV2 pathogenesis by its apoptotic activity in vivo remains to be determined. In addition, PCV2 has been demonstrated to cause lymphoid lesions in infected BALB/c mice characterized by expansion of the germinal centers in lymphoid organs with large numbers of histiocytic cells and lymphoblasts and lymphoid depletion (24), which is similar to that of PCV2-infected pigs. Therefore, this model system offers the opportunity to test the pathogenesis of mutant PCV2 that lacks expression of the ORF3 protein in vivo.

The effects of PCV2 on the immune system have been reported. Lymphopenia involving both B and T cells was demonstrable for field cases of PMWS (10, 43) and for specific-pathogen-free piglets experimentally infected with PCV2 (35), suggesting that PCV2-induced leukocytopenia was related to the lymphocyte depletion in lymphoid tissues of PMWS-affected piglets (26). Kinetic analysis of the composition of peripheral blood leukocyte populations in PCV2-infected piglets demonstrated that PCV2 infection induced primarily a lymphopenia, including depletions of $CD3^+$ $CD4^+$ $CD8^+$ memory Th, $CD3^+$ $CD4^+$ $CD8^-$ naive Th, $CD3^+$ $CD4^-$ $CD8^+$ Tc, and $CD3^+$ $CD4^-$ $CD8^-$ $\gamma\delta$ TCR^+ T lymphocytes in animals that subsequently developed PMWS (35). Altogether, these facts have led some researchers to suggest that PCV2 results in immunosuppression due to lymphocyte depletion. However, whether PCV2 could result in depletions of T-lymphocyte subsets in peripheral blood lymphocytes (PBLC) in inoculated mice, as well as ORF3 protein, and participate in the induction of cellular immunity is still unclear.

We report here that the PCV2 mutant lacking the expression of the ORF3 protein replicated efficiently and stimulates strong antibody response but was attenuated in experimentally inoculated mice without any obvious microscopic lesions. Furthermore, there are not any obvious reductions in proportions of PBLC $CD4^+$, $CD8^+$, and $CD4^+$ $CD8^+$ T-cell subsets compared to those of the control mice. On the contrary, the wild-type PCV2-inoculated mice produced lower antibody titers and showed significant decreases in the proportions of PBLC T-cell subsets after infection. Thus, these data indicate that the ORF3 protein is directly involved in viral pathogenesis via its apoptotic activity in vivo.

MATERIALS AND METHODS

Virus and cells. The permanent PK15 cell line, which was free of PCV, was maintained in minimal essential medium (MEM; Gibco) supplemented with 5% heat-inactivated fetal bovine serum (FBS), 5% L-glutamine, 100 U of penicillin G/ml, and 100 μl of streptomycin/ml at 37°C in a humidified 5% CO_2 incubator. The wild-type PCV2 virus used in the study was originally isolated from a kidney tissue sample of a pig with naturally occurring PMWS (strain BJW) (28).

Preparation and passage of mutant PCV2 in vitro. A mutant PCV2, which is absent of the expression of the ORF3 protein, was generated by transfection of PK15 cells with the mutant PCV2 infectious DNA clone as described previously (28). The mutant PCV2 virus stock was then serially passaged 15 times in PK15 cells (47). The titer of infectious virus present in the cell culture was determined by immunofluorescence analysis on PK15 cells as described previously (17) and stored at −80°C for further uses.

Experimental design. To determine the pathogenic potential of the mutant PCV2, 48 BALB/c mice aged 8 weeks old were randomly assigned to three groups. Each treatment group of mice was housed in an individual room. The 16 mice in group 1 were each inoculated with phosphate-buffered saline buffer as negative controls. Each mouse in group 2 (16 mice) and group 3 (16 mice) were inoculated both intranasally and intraperitoneally with 10^5 50% tissue culture infective doses of the PCV2 strain BJW and the mutant PCV2, respectively. The animals were monitored daily for clinical signs of disease. At 7, 14, 28, and 42 days postinoculation (dpi), four mice were randomly selected from each group and necropsied. PBLC and serum samples were collected for determining proportions of T-lymphocyte subsets, as well as the presence of PCV2 DNA and antibody, respectively. Inguinal lymph nodes, lungs, and livers were collected during necropsy and processed for histological examination and/or in situ hybridization (ISH), as well as immunohistochemical (IHC) staining.

Pathological analysis. Samples of inguinal lymph nodes, lungs, and livers were collected and fixed by immersion in 4% phosphate-buffered paraformaldehyde. Fixed samples were dehydrated, embedded in paraffin wax, and sectioned at 4 μm and then stained with hematoxylin and eosin (HE). The ISH technique to detect PCV2 nucleic acid was carried out as described previously (29), by using a PCV2-specific oligoprobe. Furthermore, an IHC technique was also used to detect the presence of viral antigen by using a polyclonal anti-PCV2 antibody according to the procedure described previously (29). Evaluation of microscopic lesions, cell apoptotic changes, and the amounts of PCV2 DNA and antigen was done in a blind fashion. Lymphoid node scores were an estimated amount of lymphoid depletion and histiocytic infiltration and/or the presence of multinucleated cells ranging from 0 (normal or no lymphoid depletion) to 3 (severe lymphoid depletion and histiocytic infiltration). Lung scores ranged from 0 (normal) to 3 (severe lymphohistiocytic interstitial pneumonia). Liver scores ranged from 0 (normal) to 3 (severe lymphohistiocytic hepatitis). Apoptotic cells were counted in six fields of view. Positive ISH results were scored as 1, 2, or 3 based on the number of positive cells labeled as PCV2 DNA. The amount of PCV2 antigen distributed in the inguinal lymph nodes was scored by assigning a score of 0 for no signal to 3 for number of positive cells.

Serology analysis. Blood samples were collected from all mice at 7, 14, 28, and 42 days after inoculation. Serum antibodies to PCV2 were detected by a modified indirect enzyme-linked immunosorbent assay (ELISA) based on the recombinant ORF2 protein of PCV2 (30). Serum samples with an optical density at 490 nm greater than those of normal mouse sera (mean ± three standard deviations) were considered seropositive for PCV2.

Quantitative real-time PCR. Quantitative real-time PCR was performed to determine the PCV2 virus loads in serum samples collected at 7, 14, 28, and 42 days after inoculation. The amplification protocol followed the instructions of a LightCycler Fast Start DNA Master^{plus} SYBR Green I kit (Roche). Briefly, the sense primer (5′-ATCAAGCGAACCACAG-3′) and the antisense primer (5′-GGTCATAGGTGAGGGGC-3′) were used to amplify a 250-bp fragment from the ORF2 gene of PCV2. Viral DNA was isolated from 100 μl of serum by using the QIAamp DNA blood minikit according to the manufacturer's instructions. The DNA extracted from serum samples was resuspended in 25 μl of DNase-RNase-proteinase-free water. The PCR parameters consisted of 40 cycles of denaturation at 94°C for 10 s, annealing at 52°C for 5 s, and extension at 72°C for 10 s. For a standard curve, serial dilutions of plasmid pBSK (PCV2 genome cloned into pBluescript SK) were used to quantify the virus genomic copy number. The geometric mean of viral genomic copies per reaction was calculated for each group after setting results for negative samples to one copy per sample. Each assay was run in duplicate.

Flow cytometry. A total of 50 μl of blood collected from each mouse was mixed with 50 μl of heparin sodium salt (50 mg/ml; Sigma). Uti-Lysed kit (Erthrocyte Lysing Reagents) (Dako) was used for lysis of erythrocytes after immunofluorescence staining according to the manufacturer's instructions. For PBLC subsets ($CD4^+$ or $CD8^+$ T lymphocyte) analysis, the heparinized blood was incubated with rat anti-mouse CD4/L3T4 fluorescein isothiocyanate- or CD8α/Lyt-2-R-phycoerythrin-conjugated antibody (Southern Biotechnology, Birmingham, AL) in the dark at room temperature for 30 min. For $CD4^+$ $CD8^+$ T cells, the heparinized blood was simultaneously incubated these two antibodies. Irrelevant antibodies were used as background controls. Samples were then analyzed on a FACScalibur instrument (Becton Dickinson) by using WinMDI 2.8 software (Purdue University Cytometry Laboratories). For the analysis, the lymphocyte region was gated on the basis of the FSC-SSC (forward light scatter-side scatter) dot plot. This permitted the identification of the T-cell subpopulations as $CD4^+$, $CD8^+$, and $CD4^+$ $CD8^+$ T-cell subsets.

Statistical analysis. Results are presented as averages ± the standard deviations or standard errors of the means, as indicated. The data were analyzed by the analysis of variance and Duncan's multiple range test. A P value of <0.05 was considered significant.

TABLE 1. Detection of viremia in sera from inoculated and control mice by real-time PCR

Group	Inoculum	No. of mice with viremia/no. tested[a] at dpi:			
		7	14	28	42
1	PBS buffer	0/4	0/4	0/4	0/4
2	wPCV2	2/4	4/4	4/4	2/4
3	mPCV2	1/4	2/4	3/4	1/4

[a] Four mice from each group were necropsied at different time points after inoculation.

TABLE 2. Seroconversion to PCV2 antibodies in mice inoculated with wPCV2 and mPCV2

Group	Inoculum	No. of mice with PCV2 antibodies/no. tested[a] at dpi:			
		7	14	28	42
1	PBS buffer	0/4	0/4	0/4	0/4
2	wPCV2	0/4	1/4	2/4	4/4
3	mPCV2	0/4	1/4	4/4	4/4

[a] Four mice from each group were necropsied at different time points after inoculation.

RESULTS

Genetic stability of recovered virus. To determine the genetic stability of the transfectant virus in vitro, we propagated the virus in PK15 cells (15 passages), isolated whole-cell nucleic acids, and amplified the ORF1 gene (the full ORF3 gene is completely overlapping the ORF1 gene at the counterdirection in the PCV2 genome) by PCR. Sequence analysis of the cloned PCR product confirmed the expected nucleotide mutation in the ORF3 gene start codon (ATG→GTG) of the mutant virus, whereas no mutation was detected in the PCR product of the wild-type virus. In addition to determine the genetic stability of the mutant virus in vivo, mice were inoculated with this virus, and their sera were collected for ORF1 amplification by PCR. Sequence analysis of the ORF1 gene from the mutant virus revealed the presence of mutation 671T→C in serum samples collected at all different time points postinfection (data not shown). As expected, no nucleotide mutation was detected in the site of the serum materials infected with the wild-type virus. These results clearly demonstrate that the mutant virus replicated in the inoculated mice but did not revert to the parent PCV2.

PCV2 mutant exhibited reduced virus loads in sera of inoculated mice. Serum samples were collected from all control and inoculated mice at 7, 14, 28, and 42 dpi and assayed for PCV2 viremia by quantitative real-time PCR and for anti-PCV2 antibody by ELISA. Negative-control animals were negative for PCV2 viremia throughout the study (Table 1). In the group 2 mice inoculated with the wild-type PCV2 (wPCV2), viremia was first detected in two of four mice at 7 dpi, followed by four of four mice at 14 and 28 dpi and then decreased for two of four mice at 42 dpi (Table 1). In group 3 mice that were inoculated with the mutant PCV2 (mPCV2), viremia was first detected in one of four mice at 7 dpi, followed by two of four mice at 14 dpi and three of four mice at 28 dpi, and only one was detected in four mice at 42 dpi (Table 1). In addition, the PCV2 genomic copy numbers per 0.1 ml of the maximum loads in serum sample for each group ranged from 2.23×10^3 to 4.82×10^4 copies in the wPCV2-inoculated mouse and from 1.35×10^3 to 2.32×10^4 copies in the mPCV2-inoculated mouse. The PCV2 load was higher in mice inoculated with the wPCV2 than in mice inoculated with the mPCV2. The differences between both groups were significant ($P < 0.05$) at 7, 14, 28, and 42 days after viral inoculation. PCV2 load dynamics during the experiment are shown in Fig. 1. Maximum levels were found at 28 dpi for mouse of the wPCV2- and mPCV2-inoculated groups.

Negative control mice were negative for anti-PCV2 antibody throughout the study (Table 2). In group 2 mice that were inoculated with the wPCV2, seroconversion to antibody of PCV2, assayed by a ORF2-specific ELISA, was first detected at 14 dpi with 1 of 4 mice, by 42 dpi, all of the 4 rest mice had seroconverted to PCV2 (Table 2). In group 3 mice that were inoculated with the mPCV2, seroconversion to PCV2 ORF2-specific antibody first occurred at 14 dpi with 1 of 4 mice, but by 28 dpi, all of the rest mice had seroconverted to PCV2 ORF2-specific antibody (Table 2). PCV2 ORF2-specific antibody dynamics during the experiment are shown in Fig. 2. The mutant virus induced ORF2-specific antibodies that were higher than those induced by the wild-type PCV2 by 14 days after inoculation. This result indicates that the mutant virus, which is deficient in producing ORF3 protein, does not result

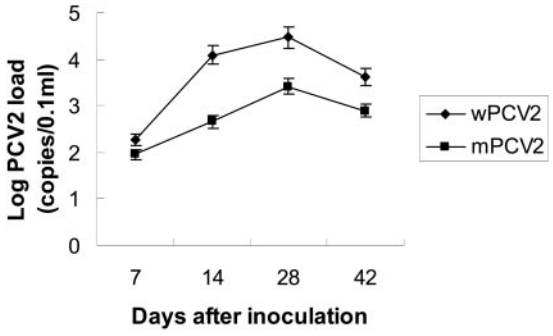

FIG. 1. Quantification of PCV2 viremia in serum by real-time PCR. The values represented are the means of the results for the four mice in each group; error bars show the standard deviations.

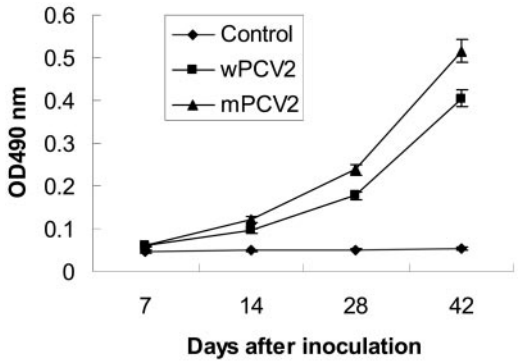

FIG. 2. PCV2 ORF2-specific antibody dynamics in mice inoculated with wPCV2 and mPCV2 by using an indirect ELISA.

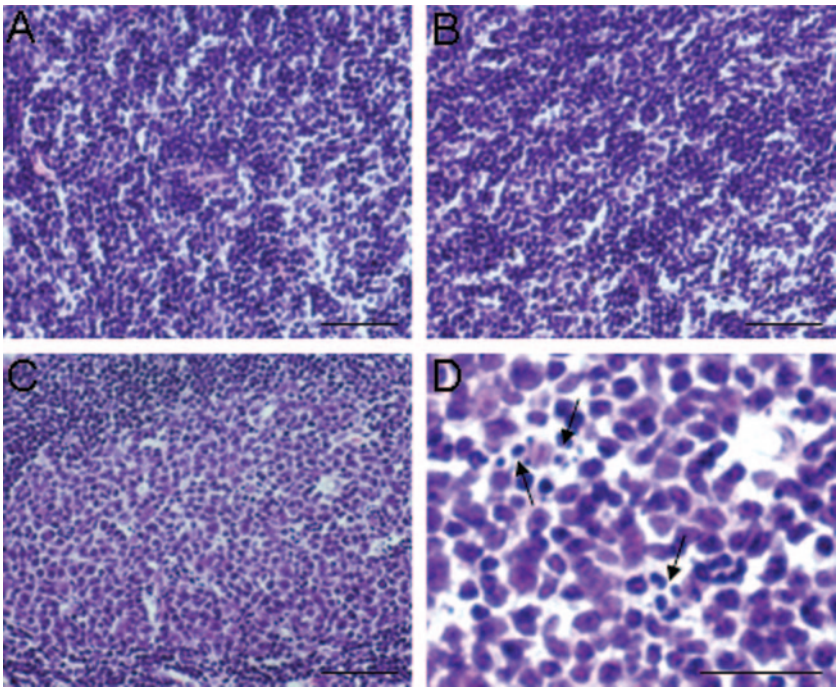

FIG. 3. Histopathologic appearance of sections (hematoxylin and eosin) of inguinal lymph nodes derived from mock-inoculated and inoculated mice at 14 dpi. (A) Normal morphology of inguinal lymph node section from an uninoculated mouse shows no noticeable germinal centers. (B) The inguinal lymph node from a mouse inoculated with the mPCV2 virus is normal and cannot be differentiated from their control counterparts. (C) Prominent germinal centers were seen in most of the parenchyma of lymph nodes of mice inoculated with the wPCV2. (D) Same germinal center in inguinal lymph node as in panel C, showing large numbers of apoptotic cells (arrows) in germinal centers. Bars, 200 μm.

in a reduced humoral immune response to PCV2 in the mouse model.

Microscopic lesions. As expected, no clinical signs or gross lesions were observed in the wild-type or mutant PCV2-inoculated mice at any time throughout the study. Inguinal lymph nodes, livers, and lung samples were further collected from all control and inoculated mice at 7, 14, 28, and 42 dpi for microscopic observation. No microscopic lesions were detected in the uninoculated control group 1 mice at any day postinoculation. Microscopic lung lesions characterized as mild peribronchiolar, lymphoplasmacytic, and histiocytic bronchointerstitial pneumonia were only observed in two of the four wPCV2-inoculated mice at 28 day postinoculation (data not shown). In the mutant-inoculated animals, no microscopic lesions were observed in the lungs. Microscopic inguinal lymph node alterations in the wPCV2-inoculated mice were first noticed at 7 dpi, prominent at 14 dpi, and most severe at 28 dpi but had started to recover by 42 dpi. At 14 dpi, wPCV2-inoculated mice exhibited prominent germinal centers that occupied most of the parenchyma in the lymph nodes (Fig. 3). These enlarged germinal centers consisted of large lymphoblastic cells and histiocytic cells. Large numbers of histiocytic cells in the germinal centers had fragmentation changes typical of apoptosis (Fig. 3). The paracortex had mild to moderate loss of lymphocytes and was infiltrated by large numbers of histiocytes. At 28 dpi, severe lymphoid depletion and histiocytic replacement were observed (data not shown). At 42 dpi, lymphocytes had partially regenerated, and lesions were slightly less severe (data not shown). In contrast, no or mild lymphoid depletion and histiocytic replacement (Fig. 3 and data not shown) were observed in the inguinal lymph nodes of the mPCV2-inoculated mice at various time points postinoculation. Mild lymphoplasmacytic hepatitis was observed in two of the four wPCV2-inoculated mice at 28 dpi (data not shown). No lymphoplasmacytic hepatitis was observed in the mutant-inoculated mice. Lesions in other tissues were unremarkable regardless of wild-type or mutant PCV2-inoculated mice.

Microscopic lesions in the lung, liver, and inguinal lymph nodes were scored (Fig. 4A and data not shown). Mean scores of lesions in the lymph nodes in mice from the mPCV2-inoculated group 3 were similar to that from group 1 but were significantly different ($P < 0.05$) from those of the wPCV2-infected group 2 mice at various time points postinoculation. The mean scores of lesions in lung and liver in mice of the wild-type PCV2-infected group 2 at 28 dpi were statistically different ($P < 0.05$) from those in group 1 and 3 mice (data not shown). At other time points dpi, the mean scores of the lung and liver lesions in mice of the two PCV2-infected groups were not statistically different from those of control mice (data not shown).

Furthermore, the apoptotic cells were also quantified in a blinded fashion, and the result is shown in Fig. 4B. The percentage of apoptotic cells in the group inoculated with the wPCV2 was significantly higher than that inoculated with the mPCV2 at various time points postinoculation, respectively. These results indicated that PCV2-induced cell death is apparently reduced due to the absence of ORF3 protein expression.

Detection of PCV2 nucleic acid and antigen. ISH staining of PCV2 nucleic acid, as well as IHC staining of PCV2 and its ORF3 antigens, was performed on inguinal lymph nodes of all

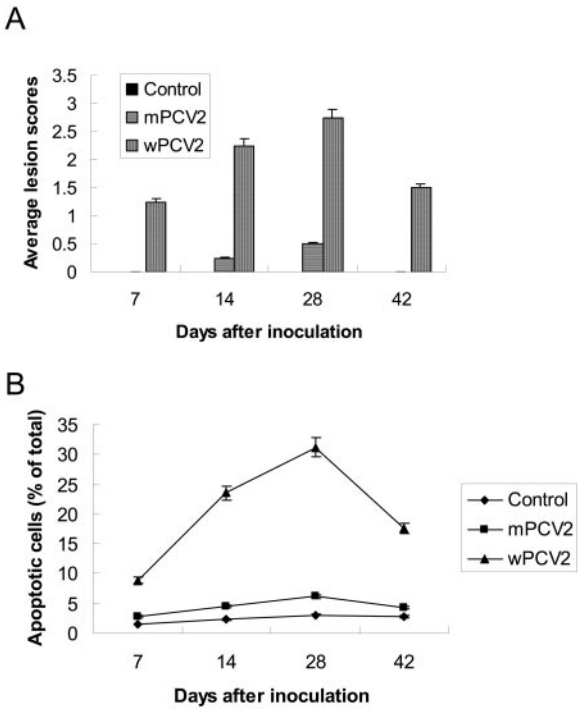

FIG. 4. (A) Evaluation of histopathological lesions in wild-type and mutant PCV2-inoculated mice. Microscopic lesions (± the standard deviation) in the inguinal lymph nodes. The data show the mean scores of four mice in each group. (B) Quantification of apoptosis induced by the wild-type and mutant PCV2 after inoculation. Apoptotic cells in the inguinal lymph nodes were determined by morphological observation; each field for the cells counted was randomly chosen with blinding to morphological results. The data show the average percentage of apoptosis of four mice in each group.

mice necropsied at 7, 14, 28, and 42 dpi. For ISH, lymph nodes from the uninoculated control mice were negative for PCV2 nucleic acid. In the wPCV2-inoculated mice, PCV2 nucleic acid was detected in two of four mice at 7 dpi, four of four mice at 14 and 28 dpi, and two of four mice at 42 dpi. In the inguinal lymph nodes, large to intermediate amounts of viral nucleic acid were detected primarily in the cytoplasm of cells with macrophages, histiocytic inflammatory cells, and syncytia (Fig. 5A and data not shown). Small round cells, which morphologically resembled lymphocytes, showed sporadic cytoplasmic labeling. Positive cells had a dark brown or black reaction product, and there was no background staining. In the mPCV2-inoculated mice, PCV2 nucleic acid was detected in one of four mice at 7 dpi, two of four mice at 14 dpi, three of four mice at 28 dpi, and one of four mice at 42 dpi. At various time points dpi, the mean scores for the estimated level of PCV2 nucleic acid in the mPCV2-inoculated animals were significantly different ($P < 0.05$) from those for the wild-type PCV2-inoculated mice, as well as control mice (Fig. 5B). In addition, PCV2 nucleic acid was also detected in the lungs and livers of some mice inoculated with the wild-type or mutant PCV2 after inoculation (data not shown).

For PCV2 antigen detection by ICH, lymph nodes from the uninoculated control mice were negative for PCV2 antigen. In group 2 mice inoculated with the wPCV2, low to high levels of PCV2 antigen were detected in the inguinal lymph nodes of each two of four mice at 7 dpi, four of four mice at 14 and 28 dpi, and two of four mice at 42 dpi. The cells labeled in lymph tissues were mainly histiocytic cells and macrophages, but cells with the morphology of lymphocytes were also labeled (Fig. 6A and data not shown). PCV2 antigen was most frequently seen in the cytoplasm of cells. Nuclear labeling was less commonly seen but occasionally appeared to be almost as abundant as cytoplasmic labeling. Weak cytoplasmic labeling was seen frequently in syncytia. In group 3 mice inoculated with the mPCV2, low to moderate levels of PCV2 antigen were detected in the inguinal lymph tissues of one of four mice at 7 dpi, two of four mice at 14 dpi, three of four mice at 28 dpi, and one of four mice at 42 dpi. At various time points dpi, the mean scores for the estimated level of PCV2 antigen in the mPCV2-inoculated animals were significantly different ($P < 0.05$) from those for the wPCV2-inoculated and control mice (Fig. 6Ba). Furthermore, PCV2 antigen was also detected in the lungs and livers of some mice inoculated with the wild-type or mutant PCV2 after inoculation (data not shown).

As expected, the inguinal lymph tissues from the control and mutant PCV2-inoculated mice were negative for ORF3 antigen at various time points postinoculation (Fig. 6A and data not shown). In contrast, ORF3 antigen was detected in lymph tissues of each two of four mice at 7 dpi, four of four mice at 14 and 28 dpi, and two of four mice at 42 dpi. ORF3 antigen was detected primarily within macrophages and histiocytic cells, as well as giant cells. ORF3 protein expression was most frequently seen in the cytoplasm but less commonly seen in the nuclear of cells (Fig. 6A). The level of ORF3 expression peaked at 14 dpi but thereafter decreased (Fig. 6Bb).

T-lymphocyte subsets. Flow cytometry was used to determine the relative proportions of $CD4^+$, $CD8^+$, and $CD4^+$ $CD8^+$ (double-positive) cell subsets in PBLC of all mice at 7, 14, 28, and 42 dpi. The results for these cell subsets were compared among groups (Table 3). With regard to the $CD4^+$ cell subset, the mean relative proportions of the wPCV2-inoculated group at 14 and 28 dpi were significantly lower ($P < 0.05$) from those for mPCV2-inoculated animals, as well as control animals, but did not differ from those from these two groups at 7 and 42 dpi. The relative proportions of $CD4^+$ cells in the mPCV2-inoculated mice did not show a significant downshift compared to that of the control group regardless of various time points after inoculation. When the relative proportions of $CD8^+$ cells were compared among groups, a significant reduction was observed for the wPCV2-inoculated group ($P < 0.05$) at 7, 14, 28, and 42 dpi but not observed for the mPCV2-inoculated group at any time points after inoculation compared to that of the control group. As for $CD4^+CD8^+$ cells, the wPCV2-inoculated animals had lower proportions of these cells than animals in the control group ($P < 0.05$) at 28 dpi only, but the mPCV2-inoculated animals had no reduction in the relative proportions of these cells at any time points after inoculation compared to that of the control group.

DISCUSSION

We previously showed that the ORF3 protein was not essential for PCV2 replication in cultured PK15 cells and played a major role in virus-induced apoptosis (28). In the present study, we used an ORF3 protein-deficient virus to study the function of ORF3 protein in vivo and demonstrated that the

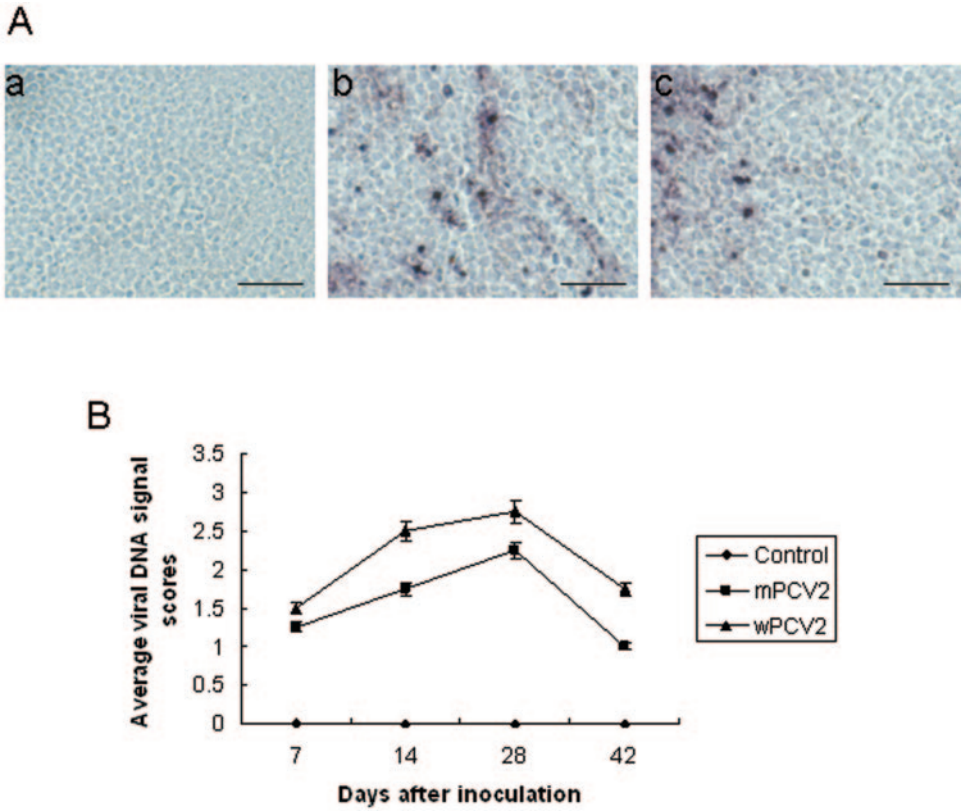

FIG. 5. (A) ISH staining of inguinal lymph node sections of mice with wPCV2 or mPCV2 at 14 dpi. Hybridization signals for PCV2 nucleic acids are purple. (a) Lymph node section from a normal mouse. No positive signals were observed. (b) wPCV2-inoculated group. Many hybridization signals were seen in most fields. (c) mPCV2-inoculated group. Reduced numbers of cells that stain for PCV2 nucleic acids were observed. Bar, 80 μm. (B) ISH detection of PCV2 nucleic acid in inguinal lymph nodes of wPCV2- and mPCV2-inoculated mice. Positive signals in ISH were scored as 1, 2, or 3 based on the amount of labeled PCV2 DNA. The data show the average scores of four mice in each group.

mutant virus can replicate in inoculated mice but does not induce any obvious lesions. This finding implies that ORF3 protein is directly involved in viral pathogenesis since the parent PCV2, expressing the ORF3 protein, was able to elicit pathological response in the mouse model.

To date, little information is available on the host range of PCV, but antibodies were found in various species other than pigs, including humans, mice, and cattle (34, 45). Kiupel et al. (24) further demonstrated that PCV2 was capable of replicating in BALB/c mice and caused microscopic lesions which are similar to that of PCV2 infection in pigs. In contrast, Quintana et al. (39) reported that no microscopic lesions compatible with PCV2 infections in pigs were detected in inoculated mice, but it is considered to be due to the dosage of the inoculum and administration route (39). In the present study we have demonstrated that inoculation of 8-week-old BALB/c mice with wPCV2 induced lymphoid node lesions, including histiocyte infiltration and lymphocyte depletion via both intranasal and intraperitoneal routes as described elsewhere (24) and thus used mice as an animal model for evaluating wPCV2 and mPCV2 infections in vivo. The histopathological analysis showed that the intensity of lesions in the inguinal lymph node tissues was related to the apparent amounts of viral DNA and antigen in those tissues, as well as virus loads in serum. In contrast, the mutant virus, which lacks ORF3 protein expression induced no obvious pathological lesions, low levels of viremia, and slightly low levels of viral DNA and antigen in lymphoid tissues with the same inoculation dose as that in the wild-type PCV2-inoculated mice. These results suggested that the mutant PCV2 is attenuated in virulence in vivo. However, the mutant virus replicated efficiently and induced stronger immune response against PCV2 compared to wild-type PCV2 (Fig. 2 and Table 2), which might be related to no reduction in $CD4^+$ T lymphocytes of mPCV2-inoculated animals (Table 3). We also showed that lack of detectable PCV2 viremia in sera or viral DNA and antigen in lymphoid tissues in some of the mPCV2-inoculated animals did not affect seroconversion to antibody against PCV2 ORF2 protein, which is in agreement with other studies (18, 19). The virus recovered from the blood of inoculated mice retained the mutation that ablated the ORF3 protein expression (data not shown), confirmed further that the ORF3 protein is also dispensable for virus replication in vivo.

PCV2 replicates in the lymph nodes, lungs, and livers of infected pigs, followed by the impairment of the immune system by degradation of the lymphoid structures (1, 2, 15, 21, 23, 48), as well as changes in the proportions of lymphocyte subsets of peripheral blood (11). In the present study, we showed that the depletion of $CD4^+$ and $CD8^+$ T cells by the wild-type virus might contribute to higher viral load of the wild-type virus

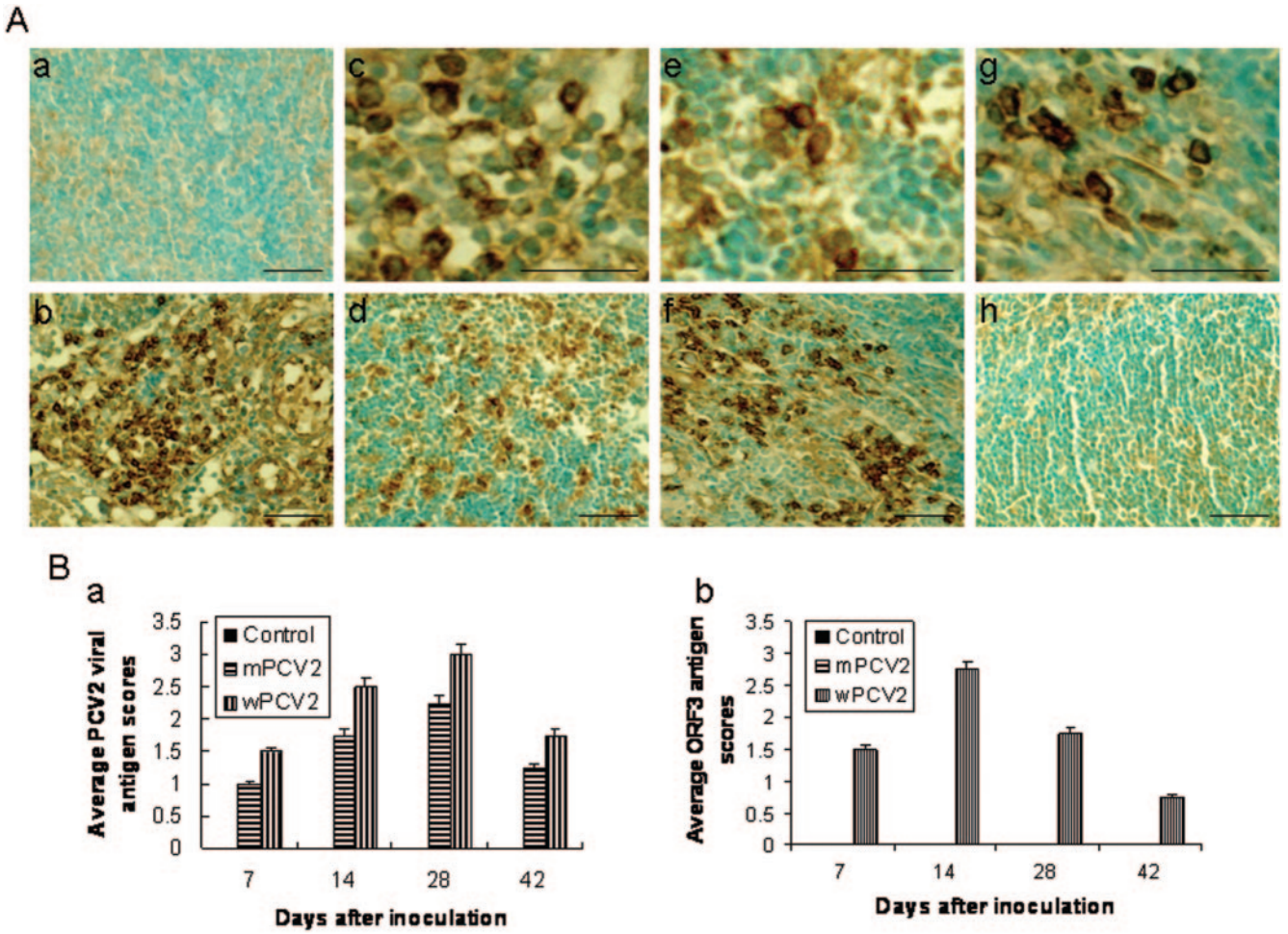

FIG. 6. (A) ICH staining of inguinal lymph node sections of mice inoculated with wPCV2 or mPCV2 at 14 dpi. PCV2 antigen-positive or ORF3-expressed cells are brown. (a) Lymph node section from a normal mouse. No staining is observed. (b) wPCV2-inoculated mouse. Many positive cells for PCV2 antigen are seen. (c) Partial enlargement of panel b. (d) mPCV2-inoculated mouse. Reduced positive cells for PCV2 antigen are seen. (e) Partial enlargement of panel d. (f) wPCV2-inoculated mouse. Many positive cells for ORF3 protein expression are seen. (g) Partial enlargement of panel f. (h) mPCV2-inoculated mouse. No staining for ORF3 protein expressing is seen. Bar, 80 μm. (B) Evaluation of PCV2 antigen and ORF3 protein expression of inguinal lymph nodes in wPCV2- and mPCV2-inoculated mice by ICH detection. PCV2-specific antigen (a) or ORF3 protein expression (b) were scored in a blinded fashion by assigning a score of 0 for no signal to 3 for a strong positive signal. The data show the mean scores of four mice in each group.

TABLE 3. Percentages of peripheral blood lymphocyte subsets in wPCV2 and mPCV2-inoculated mice

Group	Inoculum	dpi	Percentage of indicated lymphocyte[a] (mean ± SD)		
			$CD4^+$	$CD8^+$	$CD4^+$ $CD8^+$
1	PBS	7	20.3 ± 7.5^A	11.5 ± 3.2^A	3.3 ± 1.1^A
		14	21.9 ± 2.5^A	10.5 ± 3.1^A	3.4 ± 0.9^A
		28	16.8 ± 2.6^A	12.3 ± 2.1^A	3.2 ± 1.2^A
		42	15.6 ± 2.1^A	9.2 ± 1.7^A	3.5 ± 1.1^A
2	wPCV2	7	15.7 ± 2.7^A	6.2 ± 1.3^B	2.2 ± 0.9^A
		14	10.3 ± 3.3^B	4.9 ± 1.6^B	2.8 ± 0.8^A
		28	8.7 ± 2.3^B	3.1 ± 1.9^B	1.2 ± 0.6^B
		42	16.1 ± 3.1^A	5.3 ± 1.2^B	3.1 ± 1.1^A
3	mPCV2	7	18.9 ± 5.2^A	12.1 ± 3.5^A	2.7 ± 0.6^A
		14	18.7 ± 3.8^A	9.8 ± 2.6^A	3.2 ± 0.9^A
		28	16.2 ± 3.1^A	12.4 ± 3.3^A	3.6 ± 1.4^A
		42	14.6 ± 2.5^A	9.6 ± 2.1^A	2.6 ± 0.7^A

[a] Values followed by the same superscript letter (A or B) are statistically similar, while different letters for values within the same lymphocyte subset indicate significant differences in the mean values ($P < 0.05$).

compared to the mutant virus. In addition, $CD4^+$ $CD8^+$ T cells were also downshifted in the wPCV2-inoculated mice at 28 dpi, which is consistent with findings for of the PCV2-positive pigs (10). It has been reported that depletion of $CD3^+$ $CD4^+$ $CD8^+$ memory/activated Th lymphocytes was particularly discernible in the PCV2-infected piglets displaying symptoms of PMWS over time (35). In contrast, the mutant virus lacking ORF3 protein expression did not induce any obvious changes in proportions of $CD4^+$, $CD8^+$, and $CD4^+$ $CD8^+$ T cells at various time points during mPCV2 infection when inoculated into mice, indicating that the mutant virus replicates primarily in the secondary lymphoid organs of inoculated mice but causes no lymphocyte depletion and subsequently induces no damage in cell-mediated immunity due to retaining T-lymphocyte subset populations of PBLC.

Virus-induced lymphopenia has been observed in many viral infections (49), suggesting that common mechanisms proposed to explain this are related to the apoptosis of virus-specific

$CD8^+$ T cells. Induction of apoptosis of immune system cells might be one of the requirements for virus-induced immunosuppression (12). In the present study, we showed that the mutant PCV2, which lacks ORF3 protein expression, does not result in lymphocyte depletions in lymphoid tissues and any obvious apoptotic morphological changes, although it retains its ability to replicate efficiently in inoculated mice. In addition, kinetic analysis of T-lymphocyte subsets in PBLC also demonstrated that the mutant occasionally induces mild reductions in the proportions of these T-cell subsets compared to control mice. These results suggest that the mutant virus does not induce immunosuppression in inoculated animals due to the absence of apoptosis, although this needs to be further confirmed using pig infection. The induction of virus-specific cytotoxic T-lymphocyte responses is considered a key objective of vaccine development strategies (22, 41, 42). Therefore, the immunization of animals with this mutant virus strain might serve as a novel effective vaccine for inducing protection against challenges with pathogenic PCV2 strains compared to two other attenuated live strains (18, 19). However, the immune mechanism responsible for this potent vaccine-induced protection needs to be further experimentally evaluated.

Recent research suggests that nonstructural (NS) proteins do play an important role in virus-induced apoptosis and/or pathogenesis. In infectious bursal disease virus, the NS protein VP5 was also not required for viral replication in vitro and in vivo, and this protein-deficient virus did not cause bursal lesions in vivo (50) and was involved in viral pathogenesis via its apoptotic activity (51). La Crosse virus nonstructural protein NSs has been shown to induce apoptosis (9), and rLACVdelNSs mutant virus, which is deficient in expression of the NSs protein, exhibited a turbid-plaque phenotype and a less-pronounced shutoff and induced little apoptosis but still replicated efficiently, suggesting that the NSs protein could play a role in virulence (5). Within the *Circoviridae* family, 14-kDa NS protein (VP3) of chicken anemia virus was shown to cause apoptosis in lymphoblastoid T cells, and this suggested the possibility that the VP3 protein was involved in viral pathogenesis (36). In a previous study (28), we showed that the NS ORF3 of PCV2 was not required for viral replication and played a major role in virus-induced apoptosis in vitro. The results of the present study further demonstrate that the ORF3 protein is directly involved in viral pathogenesis via its apoptotic activity in vivo, as confirmed by significant reduction in PCV2-induced apoptotic cells due to the absence of the ORF3 protein expression.

In conclusion, these results show that the mutant virus, which lacks ORF3 protein expression, does not induce any obvious lesions but still replicates efficiently in a mouse model and results in a slight reduction in the proportions of T lymphocytes in PBLC different from that of the wild-type PCV2, thus demonstrating that the ORF3 protein plays an important role in viral pathogenesis via its apoptotic activity. Therefore, the generation of such ORF3 protein-deficient viruses will result in insignificant loss of lymphocytes and facilitate the development of live-attenuated vaccine for PCV2 infection.

ACKNOWLEDGMENTS

We thank Ling Eng Ang and Mdm Ng Geok Lan, Anatomy Department of the National University of Singapore, for their generous help.

This study was supported by a grant from the Temasek Life Sciences Laboratory, Singapore.

REFERENCES

1. **Allan, G. M., and J. A. Ellis.** 2000. Porcine circoviruses: a review. J. Vet. Diagn. Investig. **12:**3–14.
2. **Allan, G. M., S. Kennedy, F. McNeilly, J. C. Foster, J. A. Ellis, S. J. Krakowka, B. M. Meehan, and B. M. Adair.** 1999. Experimental reproduction of sever wasting disease by coinfection of pigs with porcine circovirus and porcine parvovirus. J. Comp. Pathol. **121:**1–11.
3. **Allan, G. M., F. McNeilly, J. P. Cassidy, G. A. Reilly, B. Adair, W. A. Ellis, and M. S. McNulty.** 1995. Pathogenesis of porcine circovirus: experimental infections of colostrum deprived piglets and examination of pig fetal material. Vet. Microbiol. **44:**49–64.
4. **Allan, G. M., F. McNeilly, S. Kennedy, B. Daft, E. G. Clarke, J. A. Ellis, D. M. Haines, B. M. Meehan, and B. M. Adair.** 1998. Isolation of porcine circovirus-like viruses from pigs with a wasting disease in the USA and Europe. J. Vet. Diagn. Investig. **10:**3–10.
5. **Blakqori, G., and F. Weber.** 2005. Efficient cDNA-based rescue of La Crosse Bunyaviruses expressing or lacking the nonstructural protein NSs. J. Virol. **79:**10420–10428.
6. **Cheung, A. K.** 2003. Transcriptional analysis of porcine circovirus type 2. Virology **305:**168–180.
7. **Choi, C., C. Chae, and E. G. Clark.** 2000. Porcine postweaning multisystemic wasting syndrome in Korean pig: detection of porcine circovirus 2 infection by immunohistochemistry and polymerase chain reaction. J. Vet. Diagn. Investig. **12:**151–153.
8. **Clark, E. G.** 1997. Post-weaning multisystemic wasting syndrome. Proc. Am. Assoc. Swine Pract. **28:**499–501.
9. **Colon-Ramos, D. A., P. M. Irusta, E. C. Gan, M. R. Olson, T. Song, R. I. Morimoto, R. M. Elliott, M. Lombard, R. Hollingsworth, J. M. Hardwick, G. K. Smith, and S. Kornbluth.** 2003. Inhibition of translation and induction of apoptosis by bunyaviral nonstructural proteins bearing sequence similarity to reaper. Mol. Biol. Cell **14:**4162–4172.
10. **Darwich, L., J. Segalés, M. Domingo, and E. Mateu.** 2002. Changes in $CD4^+$, $CD8^+$, $CD4^+$ $CD8^+$, and immunoglobulin M-positive peripheral blood mononuclear cells of postweaning multisystemic wasting syndrome-affected pigs and age-matched uninfected wasted and health pigs correlate with lesions and porcine circovirus type 2 load in lymphoid tissues. Clin. Diagn. Lab. Immunol. **9:**236–242.
11. **Darwich, L., J. Segalés, and E. Mateu.** 2004. Pathogenesis of postweaning multisystemic wasting syndrome caused by porcine circovirus 2: an immune riddle. Arch. Virol. **149:**857–874.
12. **Drew, T. W.** 2000. A review of evidence for immunosuppression due to porcine reproductive and respiratory syndrome virus. Vet. Res. **31:**27–39.
13. **Edwards, S., and J. J. Sands.** 1994. Evidence of circovirus infection in British pigs. Vet. Rec. **134:**680–681.
14. **Ellis, J., L. Hassard, E. Clark, J. Harding, G. Allan, P. Willson, J. Strokappe, K. Martin, F. McNeilly, B. Meehan, D. Todd, and D. Haines.** 1998. Isolation of circovirus from lesions of pigs with postweaning multisystemic wasting syndrome. Can. Vet. J. **39:**44–51.
15. **Ellis, J., S. Krakowka, M. Lairmore, D. Haines, A. Bratanich, E. Clark, G. Allan, C. Konoby, L. Hassard, B. Meehan, K. Martin, J. Harding, S. Kennedy, and F. McNeilly.** 1999. Reproduction of lesions of postweaning multisystemic wasting syndrome in gnotobiotic piglets. J. Vet. Diagn. Investig. **11:**3–14.
16. **Fenaux, M., P. G. Halbur, M. Gill, T. E. Toth, and X. J. Meng.** 2000. Genetic characterization of type 2 porcine circovirus (PCV-2) from pigs with postweaning multisystemic wasting syndrome in different geographic regions of North America and development of a differential PCR-restriction fragment length polymorphism assay to detect and differentiate between infections with PCV-1 and PCV-2. J. Clin. Microbiol. **38:**2494–2503.
17. **Fenaux, M., P. G. Halbur, G. Haqshenas, R. Royer, P. Thomas, P. Nawagitgul, M. Gill, T. E. Toth, and X. J. Meng.** 2002. Cloned genomic DNA of type 2 porcine circovirus is infectious when injected directly into the liver and lymph nodes of pigs: characterization of clinical disease, virus distribution, and pathologic lesions. J. Virol. **76:**541–551.
18. **Fenaux, M., T. Opriessnig, P. G. Halbur, and X. J. Meng.** 2003. Immunogenicity and pathogenicity of the chimeric infectious DNA clones between pathogenic type 2 porcine circovirus (PCV2) and non-pathogenic PCV1 in weaning pigs. J. Virol. **77:**11232–11243.
19. **Fenaux, M., T. Opriessnig, P. G. Halbur, F. Elvinger, and X. J. Meng.** 2004. Two amino acid mutations in the capsid protein of type 2 porcine circovirus (PCV2) enhanced PCV2 replication in vitro and attenuated the virus in vivo. J. Virol. **78:**13440–13446.
20. **Harding, J. C.** 1996. Post-weaning multisystemic wasting syndrome (PMWS): preliminary epidemiology and clinical presentation. Proc. West Can. Assoc. Swine Pract. **1996:**21.
21. **Harding, J. C. S., and E. G. Clark.** 1997. Recognizing and diagnosing postweaning multisystemic wasting syndrome (PMWS). Swine Health Prod. **5:**201–203.
22. **Jin, X., D. E. Bauer, S. E. Tuttleton, S. Lewin, A. Gettie, J. Blanchard, C. E.**

Irwin, J. T. Safrit, J. Mittler, L. Weinberger, L. G. Kostrikis, L. Zhang, A. S. Perelson, and D. D. Ho. 1999. Dramatic rise in plasma viremia after $CD8^+$ T-cell depletion in simian immunodeficiency virus-infected macaques. J. Exp. Med. **189:**991–998.

23. **Kennedy, S., D. Moffett, F. McNeilly, B. Meehan, J. Ellis, S. Krakowka, and G. M. Allan.** 2000. Reproduction of lesions of postweaning multisystemic wasting syndrome by infection of conventional pigs with porcine circovirus type 2 alone or in combination with porcine parvovirus. J. Comp. Pathol. **122:**9–24.
24. **Kiupel, M., G. W. Stevenson, J. Choi, K. S. Latimer, C. L. Kanitz, and S. K. Mittal.** 2001. Viral replication and lesions in BALB/c mice experimentally inoculated with porcine circovirus isolated from a pig with postweaning multisystemic wasting disease. Vet. Pathol. **38:**74–82.
25. **Kiupel, M., G. W. Stevenson, S. K. Mittal, E. G. Clark, and D. M. Haines.** 1998. Circovirus-like viral associated disease in weaned pigs in Indiana. Vet. Pathol. **35:**303–307.
26. **Ladekjær-Mikkelsen, A.-S., J. Nielsen, T. Stadejek, T. Storgaard, S. Krakowka, J. Ellis, F. McNeilly, G. Allan, and A. Bøtner.** 2002. Reproduction of postweaning multisystemic wasting syndrome (PMWS) in immunostimulated and non-immunostimulated 3-week-old piglets experimentally infected with porcine circovirus type 2 (PCV2). Vet. Microbiol. **89:**97–114.
27. **Larochelle, R., R. Magar, and S. D'Allaire.** 2002. Genetic characterization and phylogenetic analysis of porcine circovirus type 2 (PCV2) strains from cases presenting various clinical conditions. Virus Res. **90:**101–112.
28. **Liu, J., I. Chen, and J. Kwang.** 2005. Characterization of a previously unidentified viral protein in porcine circovirus type 2-infected cells and its role in virus-induced apoptosis. J. Virol. **79:**8262–8274.
29. **Liu, J. I. Chen, H. Chua, Q. Du, and J. Kwang.** Inhibition of porcine circovirus type 2 replication in mice by RNA interference. Virology, in press.
30. **Liu, C., T. Ihara, T. Nunoya, and S. Veda.** 2004. Development of an ELISA based on the baculovirus-expressed capsid protein of porcine circovirus type 2 as antigen. J. Vet. Med. Sci. **66:**237–242.
31. **Mankertz, A., M. Domingo, J. M. Folch, P. LeCann, A. Jestin, J. Segalés, B. Chmielewicz, J. Plana-Durán, and D. Soike.** 2000. Characterization of PCV2 isolates from Spain, Germany, and France. Virus Res. **66:**65–77.
32. **Mankertz, A., J. Mankertz, K. Wolf, and H. J. Buhk.** 1998. Identification of a protein essential for replication of porcine circovirus. J. Gen. Virol. **79:** 381–383.
33. **Nawagitgul, P., I. Morozov, S. R. Bolin, P. A. Harms, and S. D. Sorden.** 2000. Open reading frame 2 of porcine circovirus type 2 encodes a major capsid protein. J. Gen. Virol. **81:**2281–2287.
34. **Nayar, G. P., A. L. Hamel, L. Linn, C. Sachvie, E. Grudeski, and G. Spearman.** 1999. Evidence for circovirus in cattle with respiratory disease and from aborted bovine fetuses. Can. Vet. J. **40:**277–278.
35. **Nielsen, J., I. E. Vincent, A. Bøtner, A.-S. Ladekj(ligae)r-Mikkelsen, G. Allan, A. Summerfield, and K. C. McCullough.** 2003. Association of lymphopenia with porcine circovirus type 2 induced postweaning multisystemic wasting syndrome (PMWS). Vet. Immunol. Immunopathol. **92:**97–111.
36. **Noteborn, M. H. M., D. Todd, C. A. J. Verschueren, H. W. F. M. De Gauw, W. L. Curran, S. Veldamp, A. J. Douglas, M. S. McNulty, A. J. Van der Eb, and G. Koch.** 1994. A single chicken anemia virus protein induces apoptosis. J. Virol. **68:**346–351.
37. **Onuki, A., K. Abe, K. Togashi, K. Kawashima, A. Taneichi, and H. Tsunemitsu.** 1999. Detection of porcine circovirus from lesions of a pig with wasting disease in Japan. J. Vet. Med. Sci. **61:**1119–1123.
38. **Pringle, C. R.** 1999. Virus taxonomy at the XIth International Congress of Virology, Sydney, Australia. Arch. Virol. **144:**2065–2070.
39. **Quintana, J., M. Balasch, J. Segalés, M. Calsamiglia, G. M. Rodríguez-Arrioja, J. Plana-Durán, and M. Domingo.** 2002. Experimental inoculation of porcine circoviruses type 1 (PCV1) and type 2 (PCV2) in rabbits and mice. Vet. Res. **33:**229–237.
40. **Roulston, A., R. C. Marcellus, and P. E. Branton.** 1999. Virus and apoptosis. Annu. Rev. Microbiol. **53:**577–628.
41. **Schmitz, J. E., R. P. Johnson, H. M. McClure, K. H. Manson, M. S. Wyand, M. J. Kuroda, M. A. Lifton, R. S. Khunkhun, K. J. McEvers, J. Gillis, M. Piatak, J. D. Lifson, G. Grosschupff, P. Racz, K. Tenner-Racz, E. P. Rieber, K. Kuus-Reichel, R. S. Gelman, N. L. Letvin, D. C. Montefiori, R. M. Ruprecht, R. C. Desrosiers, and K. A. Reimann.** 2005. Effect of $CD8^+$ lymphocyte depletion on virus containment after simian immunodeficiency virus SIVmac251 challenge of live attenuated SIVmac293Δ3-vaccinated rhesus macaques. J. Virol. **79:**8131–8141.
42. **Schmitz, J. E., M. J. Kuroda, S. Santra, V. G. Sasseville, M. A. Simon, M. A. Lifton, P. Racz, K. Tenner-Racz, M. Dalesandro, B. J. Scallon, J. Ghrayeb, M. A. Forman, D. C. Montefiori, E. P. Rieber, N. L. Letvin, and K. A. Reimann.** 1999. Control of viremia in simian immunodeficiency virus infection by $CD8^+$ lymphocytes. Science **283:**857–860.
43. **Segalés, J., F. Alonso, C. Rosell, J. Pastor, F. Chianini, E. Campos, L. López-Fuertes, J. Quintana, G. Rodríguez-Arrioja, M. Calsamiglia, J. Pujols, J. Domínguez, and M. Domingo.** 2001. Changes in peripheral blood leukocyte populations in pigs with natural postweaning multisystemic wasting syndrome (PMWS). Vet. Immunol. Immunopathol. **81:**37–44.
44. **Segalés, J., and M. Domingo.** 2002. Postweaning multisystemic wasting syndrome (PMWS) in pigs: a review. Vet. Q. **24:**109–124.
45. **Tischer, I., L. Bode, J. Apodaca, H. Timm, D. Peters, R. Rasch, S. Pociuli, and E. Gerike.** 1995. Presence of antibodies reacting with porcine circovirus in sera of humans, mice, and cattle. Arch. Virol. **140:**1427–1439.
46. **Tischer, I., W. Mields, D. Wolff, M. Vagt, and W. Griem.** 1986. Studies on epidemiology and pathogenicity of porcine circovirus. Arch. Virol. **91:**271–276.
47. **Tischer, I., D. Peters, R. Rasch, and S. Pociuli.** 1987. Replication of porcine circovirus: induction by glucosamine and cell cycle dependence. Arch. Virol. **96:**39–57.
48. **Wellenberg, G. J., S. Pesh, F. W. Berndsen, P. J. Steverink, W. Hunneman, T. J. Van der Vorst, N. H. Peperkamp, V. F. Ohlinger, R. Schippers, J. T. Van Oirschot, and M. F. de Jong.** 2000. Isolation and characterization of porcine circovirus type 2 from pigs showing signs of post-weaning multisystemic wasting syndrome in The Netherlands. Vet. Q. **22:**167–172.
49. **Welsh, R. M., K. Bahl, and X. Z. Wang.** 2004. Apoptosis and loss of virus-specific $CD8^+$ T-cell memory. Curr. Opin. Immunol. **16:**271–276.
50. **Yao, K., M. A. Goodwin, and V. N. Vakharia.** 1998. Generation of a mutant infectious bursal disease virus that does not cause bursal lesions. **72:**2647–2654.
51. **Yao, K., and N. Vakharia.** 2001. Induction of apoptosis in vitro by the 17-kDa nonstructural protein of infectious bursal disease virus: possible role in viral pathogenesis. Virology **285:**50–58.